

# Sand dollar skeleton as templates for bacterial cellulose coating and apatite precipitation

A. M. Barreiro · D. O. S. Recouvreux ·  
D. Hotza · L. M. Porto · C. R. Rambo

Received: 30 November 2009 / Accepted: 27 April 2010 / Published online: 8 May 2010  
© Springer Science+Business Media, LLC 2010

**Abstract** In this work, the skeleton of Sand Dollar (*Clypeaster subdepressus*) was coated by bacterial cellulose (BC) produced by *Gluconacetobacter hansenii* and subsequently coated with calcium phosphate (apatite). The skeleton of sand dollar is composed of magnesium calcite ((Ca,Mg)CO<sub>3</sub>) and exhibits an hierarchically porous structure with interconnected porosity. After coating, the small-sized pores were partially covered by cellulose microfibrils, where apatite particles were homogeneously deposited. The pore geometry of sand dollar is adequate for bone regeneration, allows cell migration through its large cells and permit vascularization through the small pores. Moreover, BC/apatite coating offers a bioactive surface for cell adhesion.

## Introduction

Bacterial cellulose (BC) produced by several bacteria, notably by *Gluconacetobacter hansenii*, is an extra cellular polysaccharide that form long nanofibers. BC is composed of  $\beta(1 \rightarrow 4)$  glucose units forming network structures of linear chains [1–3]. Its molecular formula is identical to vegetal cellulose, but with significant differences of

structural features and properties like high purity, high degree of polymerization, high crystallinity, high water holding capability, and high mechanical stability [4]. BC also exhibits excellent biocompatibility, bioactivity, and high osteoconductivity [5, 6]. Moreover, BC nanofibrous network mimics the extracellular matrix and, therefore, it can be used for cell adhesion and proliferation in tissue engineering.

In bone tissue engineering, scaffolds serve as biointerfaces or bioactive supports that allow surrounding cells to migrate into them, and regenerate the damaged tissue. In addition to the chemical nature, the adequate micromorphology of a porous scaffold for bone substitute is characterized its porosity, as well as pore size and interconnectivity to allow cellular infiltration and ingrowth [7, 8]. Several biomaterials have been investigated for this purpose, including BC, hydroxyapatite (HAp), and combination of both, to obtain porous composite materials for tissue engineering application [9–11].

Invertebrate species such as starfish, sea urchins, natural sponges, cephalopod mollusks, and coral have been investigated for tissue engineering applications. These animals have skeletons with structural properties that make them suitable scaffolds for bone regeneration due to their porous skeleton with cellular morphologies and hierarchical structures [12, 13]. The simplest process is the direct use of the skeleton after treatment to remove immunogenic proteins, artifacts, and foreign bodies [13]. Corals are often used in bone replacement and have presented very promising results [14–16]. However, the ecological equilibrium can be affected when corals are harvested. The sand dollar skeleton has similar anatomic features to corals and could be used without affecting the habitat, as happens with corals [17]. The skeleton of sand dollar (*Clypeaster subdepressus*) exhibit interconnected porosity with pore size

A. M. Barreiro · D. O. S. Recouvreux · L. M. Porto ·  
C. R. Rambo (✉)  
Integrated Technologies Laboratory, Department of Chemical  
Engineering, Federal University of Santa Catarina,  
Florianopolis, SC, Brazil  
e-mail: rambo@intelab.ufsc.br

D. Hotza  
Group of Glass and Ceramic Materials, Department of Chemical  
Engineering, Federal University of Santa Catarina,  
Florianopolis, SC, Brazil

gradients, high surface area, thermal stability, and low weight. Interconnected pores provide a framework for bone ingrowth and ensure the nutrition and blood supply for growing tissue. Large ducts can also induce the blood vessels to branch out into the macropores [17, 18]. Araiza et al. [18] transformed an echinoderm calcite skeleton into porous HAp by treatment with phosphated boiling solutions to change its composition, maintaining the original porous microstructure.

This work reports on the use of sand dollar skeleton as templates for BC coating by *Gluconacetobacter hansenii* and in situ deposition of HAp. The BC coating process combines the bioactivity of BC and apatite with the mechanical strength and cellular microarchitecture of sand dollar skeleton.

## Materials and methods

Bacteria *Gluconacetobacter hansenii* acquired from “Collection of Tropical Culture” (CCT, André Tosello Foundation) was used for cellulose production. The bacteria inoculum was prepared in 125 mL Erlenmeyer flasks, containing 25 mL of culture medium with 3 g L<sup>-1</sup> peptone, 5 g L<sup>-1</sup> yeast extract, and 25 g L<sup>-1</sup> mannitol. The compounds were dissolved in distilled water, pH 6.6, and sterilized by autoclaving for 20 min at 120 °C. The medium was inoculated with 5% (v/v) of the bacteria stock culture [19].

Broken pieces of sand dollar skeleton were collected on the south coast of Brazil (Florianopolis, SC, 27°44'S, 48°30'W). Cubic samples of 1 cm<sup>3</sup> of the skeleton were first washed to remove excess sand, dried, and sterilized by autoclaving for 20 min at 120°C. The samples were then immersed in the bacteria culture medium in an orbital shaker (150 rpm), at 30°C, during 1 to 4 days to be coated by BC. After the cultivation period, BC-coated scaffolds were removed, washed with distilled water and dried at 50 °C. Subsequently, the scaffolds were treated with a 0.1 M NaOH solution at 90 °C for 30 min to remove bacterial impurities. The samples were again washed in distilled water until neutral pH and then dried at 50 °C for 24 h.

Calcium phosphate was precipitated on both sand dollar skeleton and on BC-coated skeleton by immersion in simulated body fluid (SBF) in which the ion concentrations were multiplied by five (5 × SBF) (Table 1). Concentrated solutions of KCl, NaCl, NaHCO<sub>3</sub>, MgSO<sub>4</sub> \* 7H<sub>2</sub>O, CaCl<sub>2</sub>,

and KH<sub>2</sub>PO<sub>4</sub> were mixed in distilled water [9, 20]. After 96 h or 120 h of SBF immersion, the samples were dried at 50 °C and the weight gain and BC layer thickness were plotted in function of BC cultivation period.

Microstructure and morphology of the samples were evaluated by scanning electron microscopy (SEM, Philips, XL-30) equipped with energy dispersive spectroscopy (EDS). Phase composition of sand dollar skeleton was determined by powder X-ray diffractometry (XRD, Philips, X'Pert, The Netherlands) using CuK<sub>α</sub> radiation. The strut density ( $\rho_s$ ) was determined by He-pycnometer (AccuPyc 1330, Micromeritics, USA) using powdered pieces of the samples. The total porosity,  $\varepsilon$ , of a set of six samples of each batch was estimated from the relation between the strut density and the geometrical density ( $\rho_G$ ), according to the expression:  $\varepsilon = (1 - \rho_G/\rho_s)$ , where  $\rho_G$  is the density of the fibrous specimen (the weight of a sample divided by the geometrical measured volume). Strength under compression of a set of 10 samples with nominal dimensions of 5 × 5 × 7 mm was determined at room temperature using a universal testing device (EMIC DL2000, Brazil). The speed of the crosshead was set constant to 1 mm/min.

## Results and discussion

Figure 1 shows SEM micrographs of the micromorphology of the sand dollar skeleton. The skeleton is comprised by open and interconnected pores (Fig. 1a) with an open porosity of 81 ± 2%. The porous cellular morphology is composed of hierarchically structured cells with a bimodal pore size distribution, where small pores of approximately 50 μm form the walls of larger ducts (~500 μm) (Fig. 1b). This anatomical feature characterizes sand dollar skeleton as adequate bone tissue scaffold to ensure nutrient exchange [21]. Pore sizes larger of 500 μm also allow cell migration (osteoblasts) and tissue ingrowth [22].

Figure 2 shows the X-ray diffractogram of the sand dollar skeleton, where the great majority of the peaks is attributed to calcite CaMg(CO<sub>3</sub>)<sub>2</sub>. Although (Ca,Mg)CO<sub>3</sub> is a bioceramic, its biocompatibility to human cells is not often reported.

When the sand dollar skeleton is introduced in the bacteria culture medium, it serves as bioinert support for cellulose synthesis. Figure 3 shows SEM images of a sand dollar skeleton coated with BC after 24 h immersion in

**Table 1** Ion concentration in SBF used for apatite deposition on BC-coated sand dollar skeleton

Ion	Na <sup>+</sup>	K <sup>+</sup>	Ca <sup>2+</sup>	Mg <sup>2+</sup>	Cl <sup>-</sup>	HCO <sub>3</sub> <sup>-</sup>	HPO <sub>4</sub> <sup>2-</sup>	SO <sub>4</sub> <sup>2-</sup>
Concentration (mmol/L)	627.0	25.0	12.5	5.0	645.0	27.0	5.0	5.0

**Fig. 1** SEM micrographs of sand dollar skeleton

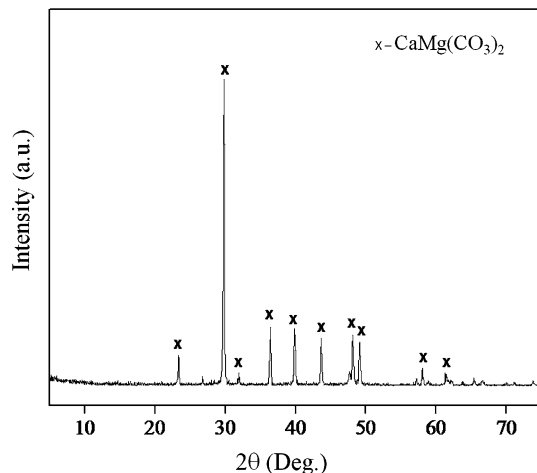
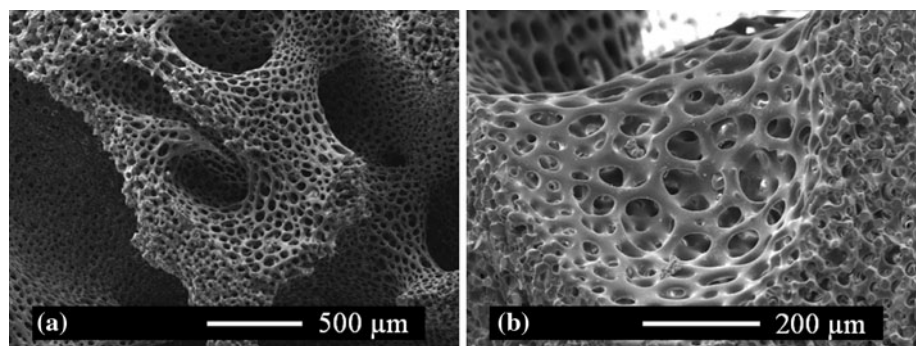


**Fig. 2** X-ray diffraction spectrum of a sand dollar skeleton

culture medium. BC layers are heterogeneously distributed inside the large ducts (Fig. 3a). The small-sized pores (Fig. 3b) were partially coated by a network of cellulose nanofibers. The cellulose produced by *G. hansenii* is synthesized by introducing glucose units to the reducing ends of the polymer resulting in long nanofibers that structurally resembles the extracellular collagen matrix. The formed composite exhibits the cellular porous morphology of the trabecular bone, coated with the nanofibrous matrix.

After 96 h immersion in SBF (Fig. 4), SEM micrographs of scaffolds submitted to different BC cultivation times revealed that cellulose nanofibers serve as supports

for deposition of apatite particles over the BC surface. For comparison Fig. 4a shows apatite deposition after 96 h on a sand dollar surface without the cellulose layer. Particles with diameters below 0.5 mm coated uniformly the entire structure. After 24 h of cultivation cellulose nanofibers partially clogged the small pores (Fig. 4b) and promoted apatite precipitation of SBF immersion (Fig. 4c). Moreover, after 48 and 72 h a layer of cellulose coated the whole sand dollar cellular structure and also allowed apatite precipitation (Fig. 4d and e, respectively). After 96 h of BC formation apatite particles precipitated and large agglomerates anchored to the cellulose fibers that coated the sand dollar skeleton (Fig. 4e), leading to a microstructure in which the apatite particles are entangled with BC nanofibers. Such scaffold construct may provide an adequate environment for cell attachment and growth. Figure 4f shows apatite precipitation after 120 h immersion in SBF and 96 h of BC cultivation. A fully coated scaffold can be seen, where a dense apatite layer coated the small pores, and the larger pores are covered by cellulose fibers. The time to achieve a homogeneous apatite coating was no shorter than 96 h on pure sand dollar skeleton. However, 120 h was required for a uniform apatite deposition on BC fibers, independently of the BC cultivation time, i.e. cellulose thickness.

The EDS analysis of the BC layer confirmed the presence of Ca and P with a Ca:P ratio of 1.47, which is lower than the Ca:P ratio for stoichiometric HAp (1.67). HAp prepared from aqueous solutions usually results in Ca:P

**Fig. 3** SEM micrographs of sand dollar skeleton after: **a** 24 h of BC coating, **b** 72 h of BC coating

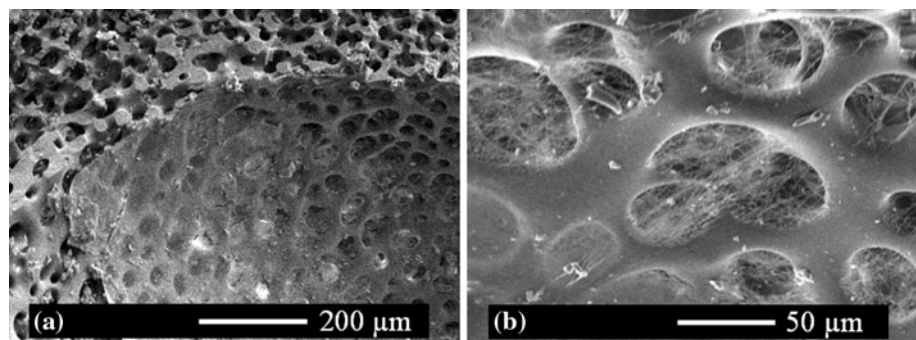
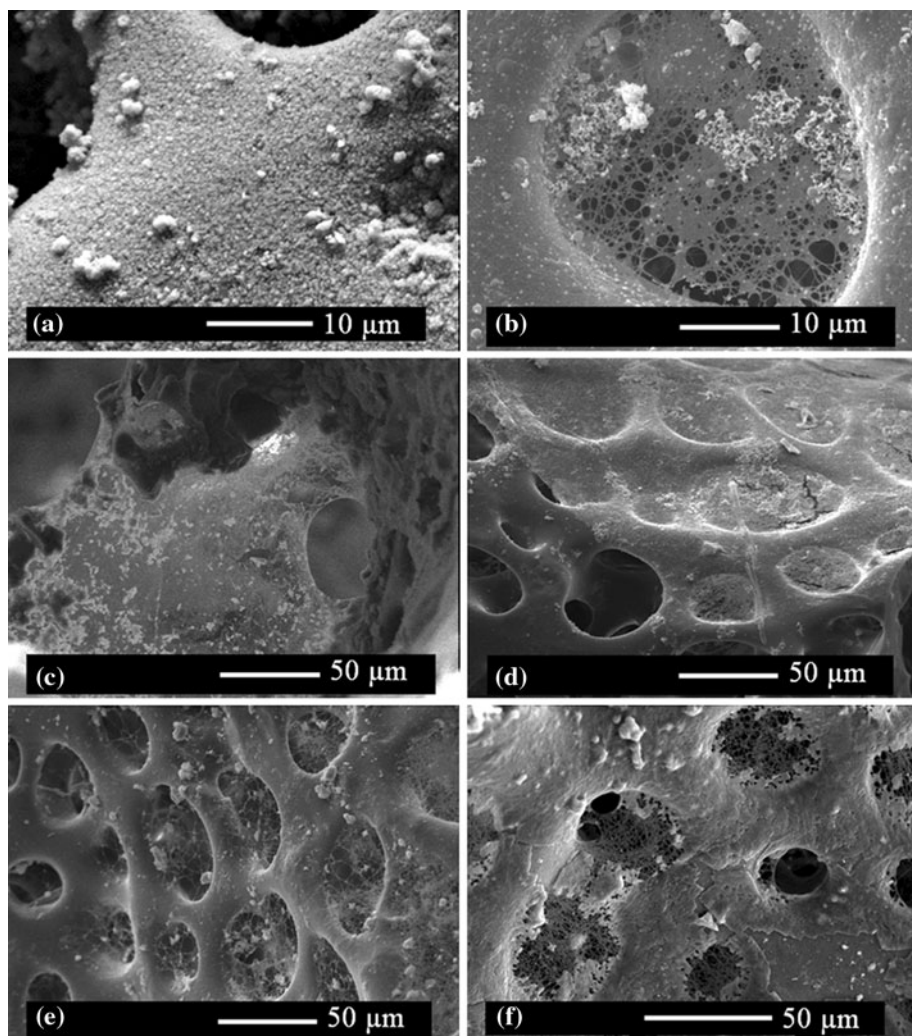


**Fig. 4** SEM micrographs of sand dollar skeleton immersed for 96 h in SBF after cellulose formation during: **a** 0 h (without cellulose), **b** 24 h, **c** 48 h, **d** 72 h, **e** 96 h, and **f** 96 h cellulose cultivation and 120 h immersion in SBF



ratios ranging from 1.33 to 1.67. Biological apatite is a non-stoichiometric Ca-deficit calcium phosphate with varied composition.

Figure 5 shows the BC layer thickness (Fig. 5a) and the weight gain (Fig. 5b) in function of BC cultivation period of sand dollar skeletons after 96 h immersed in SBF. Both curves exhibit similar behavior with respect to the period of BC culture. An increase in the thickness of the BC coating can be seen in Fig. 5b is related to the BC production by the bacteria that proliferate and excrete cellulose nanofibers until the carbon source is completely consumed. Weight increase in the samples (Fig. 5b) is directly associated to the increase of the cellulose fibers coating area and thickness. The BC mass fraction increase resulted in a higher area for apatite to attach, which consequently increased the amount of apatite particles.

The average strength under compression of the scaffolds was  $3.6 \pm 0.8$  MPa, which is adequate to be used for bone repairing therapies as temporary bone parts substitutes. The

compressive strength of the sand dollar based scaffolds is to the human tibial cancellous bone [23].

Despite the suitable features of BC-coated and apatite precipitated sand dollar skeleton for applications in bone tissue regeneration, the developed processing route does not make use of heat treatments or solvents that could leave toxic residues.

## Conclusion

Sand dollar was used as templates for BC coating and apatite precipitation. The cellular geometry of sand dollar is adequate for bone regeneration, allows cells migration through the large cells, and permit vascularization through the small pores. Cellulose layer thickness and weight increased with culture time. Precipitation of calcium phosphate on BC layer offers a biotolerant surface for cell adhesion and could be useful in bone tissue regeneration.

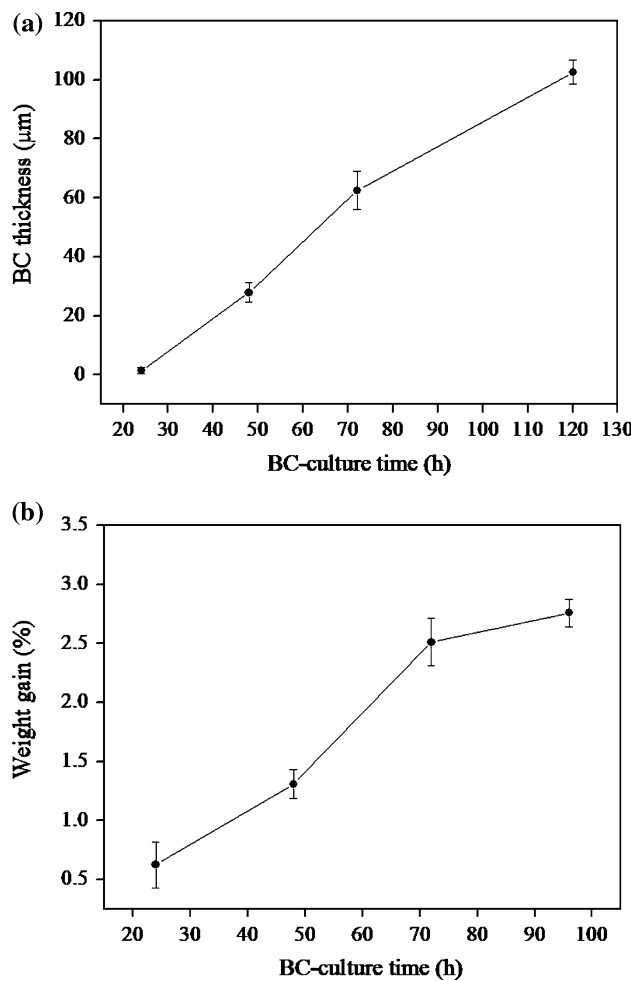


**Fig. 5** Weight gain (a) and BC thickness (b) after 96 h in SBF solution in function of BC coating period

**Acknowledgements** The authors thank the Conselho Nacional de Desenvolvimento Científico e Tecnológico (CNPq) and Coordenação de Aperfeiçoamento de Pessoal de Nível Superior (CAPES), Brazil for the financial support.

## References

- Rambo CR, Recouvreux DOS, Carminatti CA, Pitlovancic AK, Antônio RV, Porto LM (2008) Mater Sci Eng 28:549
- Jung JY, Park JK, Chang HN (2005) Enzym Microbiol Technol 37:347
- Ross P, Mayer R, Benziman M (1991) Microbiol Mol Biol Rev 55:35
- Wan YZ, Huang Y, Yuan CD, Raman S, Zhu Y, Jiang HJ, He F, Gao C (2007) Mater Sci Eng C 27:855
- Klemm D, Schumann D, Kramer F, Heßler N, Hornung M, Schmauder HP, Marsch S (2006) Adv Polym Sci 205:49
- Wan YZ, Hong L, Jia SR, Huang Y, Zhu Y, Wang YL, Jiang HJ (2006) Comp Sci Technol 66:1825
- Bovan BD, Hummert TW, Dean DD, Schwartz Z (1996) Biomaterials 17:137
- Green D, Walsh D, Mann S, Oreffo ROC (2002) Bone 30:810
- Rambo CR, Müller FA, Müller L, Sieber H, Hofmann I, Greil P (2006) Mater Sci Eng 26:92
- Hong L, Wang YL, Jia SR, Huang Y, Gao C, Wan YZ (2006) Mater Lett 60:1710
- Fricain JC, Granja PL, Barbosa MA, de Jéso B, Barthe N, Baquey C (2002) Biomaterials 23:971
- White E, Weber JN, Roy DM, Owen EL, Chiroff R, White AR (1975) J Biomed Mater Res 6:23
- Green DW (2008) Biomed Mater 3:034010
- Petite H, Viateau V, Bensaïd W, Meunier A, Pollak C, Bourguignon M, Oudina K, Sedel L, Guillemin G (2000) Nat Biotechnol 18:959
- Demers C, Hamdy CR, Corsi K, Chellat F, Tabrizian M, Yahia L (2002) Bio-Med Mater Eng 12:115
- Roux FX, Brasnu D, Loty B, George B, Guillemin G (1988) J Neurosurg 69(4):510
- Rodríguez-Lugo V, Camacho-Bragado GA, Castaño VM (2003) Mater Manuf Process 18(1):67
- Araiza MA, Gómez-Morales J, Clemente RR, Castaño VM (1999) J Mater Syn Proc 7(4):211
- Recouvreux DOS, Rambo CR, Carminatti CA, Berti FV, Antônio RV, Porto LM (2008) In: 21th CBEB, Salvador, BA, Brazil
- Müller FA, Müller L, Hofmann I, Greil P (2005) Key Eng Mater 183:284
- Wintermantel E, Mayer J, Blum J, Eckert KL, Liischer P, Mathey M (1996) Biomaterials 17(2):83
- Wake MC, Patrick CW, Mikos AG (1994) Cell Transplant 3:339
- Hvid I, Christensen P, Sondergaard J, Christensen PB, Larsen CG (1983) Acta Orthop Scand 54:819